Supporting Information

Counter anions influence the relaxation dynamics of phenoxy-bridged Dy_2 single molecule magnets

Shuting Liu,[a,b] Jingjing Lu,[a] Xiao-lei Li,[a] Zhenhua Zhu[a,c] and Jinkui Tang*[a,b]

[a]*State Key Laboratory of Rare Earth Resource Utilization, Changchun Institute of Applied Chemistry, Chinese Academy of Sciences, Changchun 130022, P. R. China*
[b]*School of Applied Chemistry and Engineering, University of Science and Technology of China, Hefei 230026, P. R. China*
[c]*University of Chinese Academy of Sciences, Beijing 100049, P. R. China*

Corresponding Author: Jinkui Tang
E-mail: tang@ciac.ac.cn

Table S1. Crystallographic Data and Structure Refinement for **1-4**.

Compound	**1**	**2**	**3**	**4**
Formula	$C_{53}H_{60}Cl_2Dy_2N_{12}O_{15}$	$C_{55}H_{63}Dy_2N_{14}O_{21}$	$C_{57}H_{70}Cl_2Dy_2N_{12}O_{24}$	$C_{120}H_{133}Cl_2Dy_4F_{12}N_{24}O_{39}S_4$
Formula weight	1501.03	1581.19	1703.15	3612.64
Temperature/K	173.15	173.15	173.15	173.15
Crystal system	monoclinic	monoclinic	monoclinic	triclinic
Space group	$P2_1/c$	$P2_1/c$	$P2_1/n$	$P\bar{1}$
a/Å	14.434(5)	14.515(3)	14.0961(9)	15.7602(13)
b/Å	17.950(7)	18.063(4)	18.9669(12)	18.2693(15)
c/Å	26.051(9)	27.276(7)	26.3438(18)	24.804(2)
α/°	90	90	90	95.9670(10)
β/°	93.072(8)	92.250(5)	104.9210(10)	100.081(2)
γ/°	90	90	90	90.9640(10)
Volume/Å^3	6740(4)	7146(3)	6805.8(8)	6989.1(10)
Z	4	4	4	2
ρ_{calc}/g·cm^{-3}	1.479	1.470	1.662	1.717
F(000)	2992	3164	3416	3606
Crystal size/mm^3	0.12×0.11×0.1	0.12×0.11×0.1	0.2×0.15×0.1	0.15×0.12×0.1
Reflns collected	41046	39282	26112	43444
Rint	0.0812	0.1037	0.0447	0.027
GOF on F^2	1.031	0.995	1.107	1.027
R1, wR2 [I>=2σ (I)]	0.0657, 0.1855	0.0586, 0.1368	0.0582, 0.1517	0.0400, 0.1099
R1, wR2 [all data]	0.0887, 0.2011	0.0932, 0.1544	0.0729, 0.1595	0.0479, 0.1168
CCDC number	2004686	2004687	2004688	2004689

Table S2. CShM Values of **1-4**.

central atom	coordination polyhedron	**1**	**2**	**3**	**4**
Dy(1)	Square antiprism (SAPR-8, D4d)	4.253	4.009	4.275	4.112
	Triangular dodecahedron (TDD-8, D2d)	**3.447**	**3.499**	**3.844**	**3.895**
	Biaugmented trigonal prism J50 (JBTPR-8, C2v)	4.839	4.762	4.793	4.934
	Biaugmented trigonal prism (BTPR-8, C2v)	3.952	3.76	3.943	4.157
	Snub diphenoid J84 （JSD-8, D2d)	5.684	5.775	5.823	5.872
Dy(2)	Square antiprism (SAPR-8, D4d)	4.335	4.361	4.26	4.592
	Triangular dodecahedron (TDD-8, D2d)	4.455	4.061	4.118	4.556
	Biaugmented trigonal prism J50 (JBTPR-8, C2v)	5.144	5.214	5.221	5.342
	Biaugmented trigonal prism (BTPR-8, C2v)	4.32	4.533	4.451	4.549
	Snub diphenoid J84 （JSD-8, D2d)	6.262	5.854	6.088	6.346

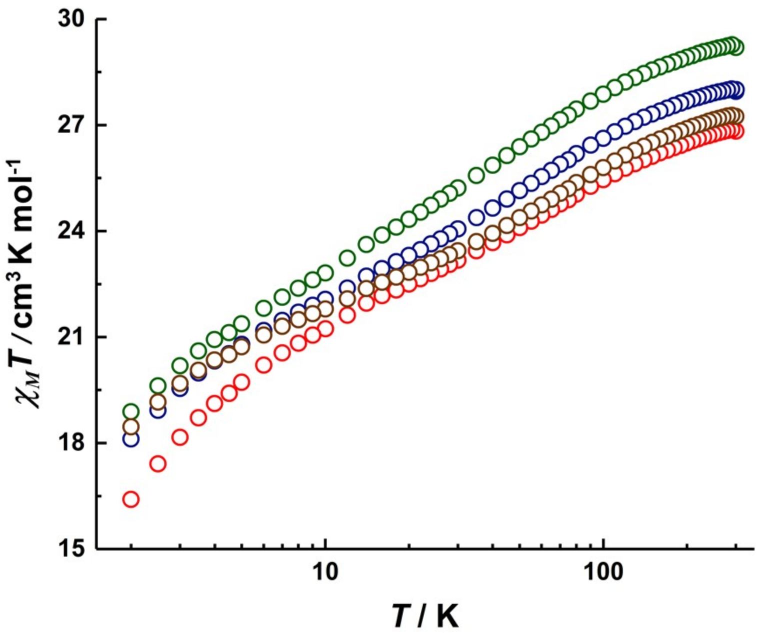

Figure S1. Temperature dependence of the $\chi_M T$ values at 1000 Oe for **1** (red), **2** (blue), **3** (green) and **4** (brown) with the x axis in log scale to highlight the low temperature magnetic properties.

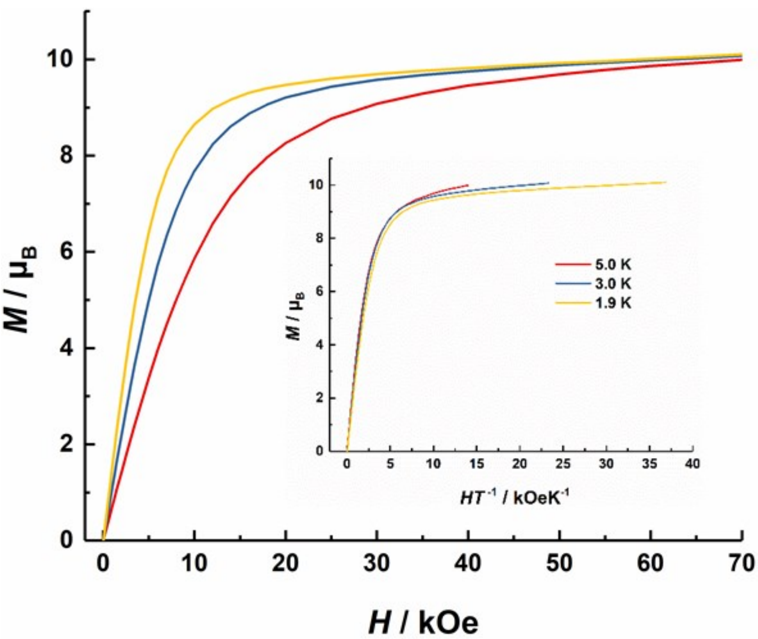

Figure S2. Field dependence of magnetization for **1**. Inset: *M* versus *H/T* plot for **1**.

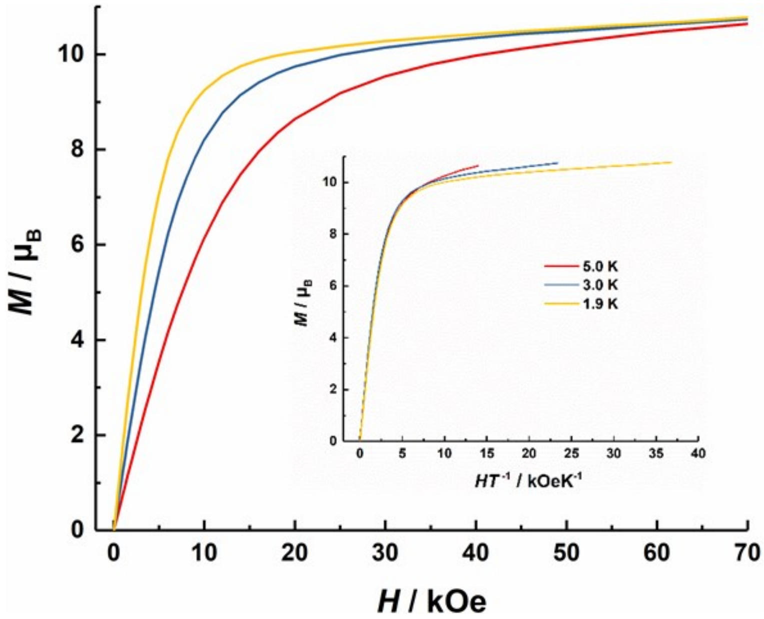

Figure S3. Field dependence of magnetization for **2**. Inset: *M* versus *H/T* plot for **2**.

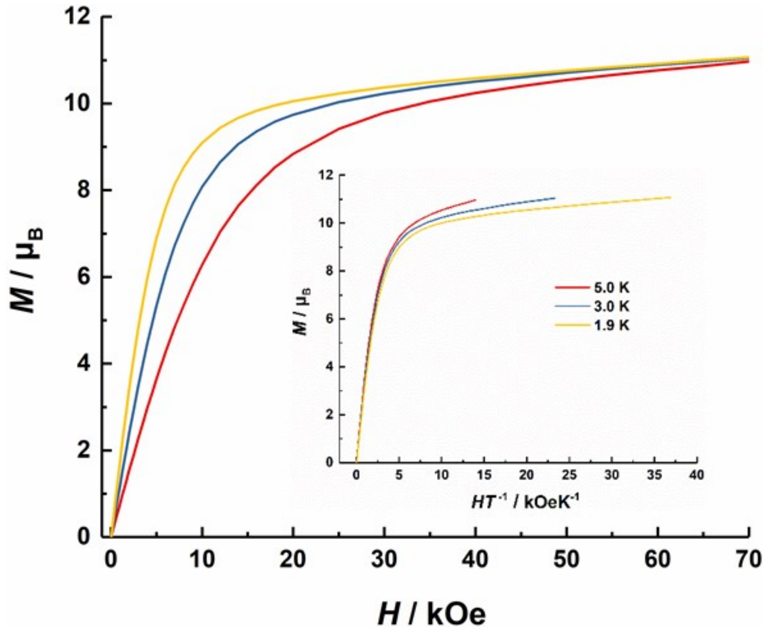

Figure S4. Field dependence of magnetization for **3**. Inset: *M* versus *H/T* plot for **3**.

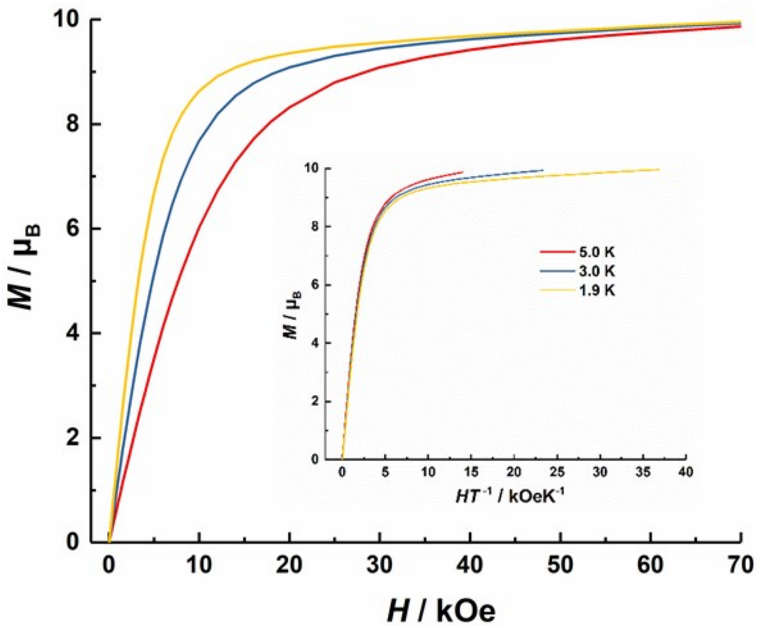

Figure S5. Field dependence of magnetization for **4**. Inset: *M* versus *H/T* plot for **4**.

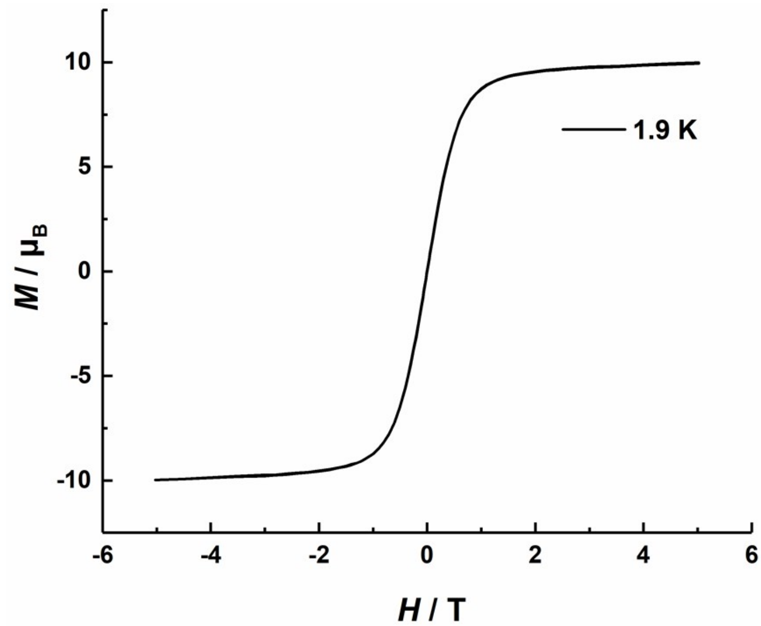

Figure S6. Variable magnetic field magnetization measurement for **1** at 1.9 K.

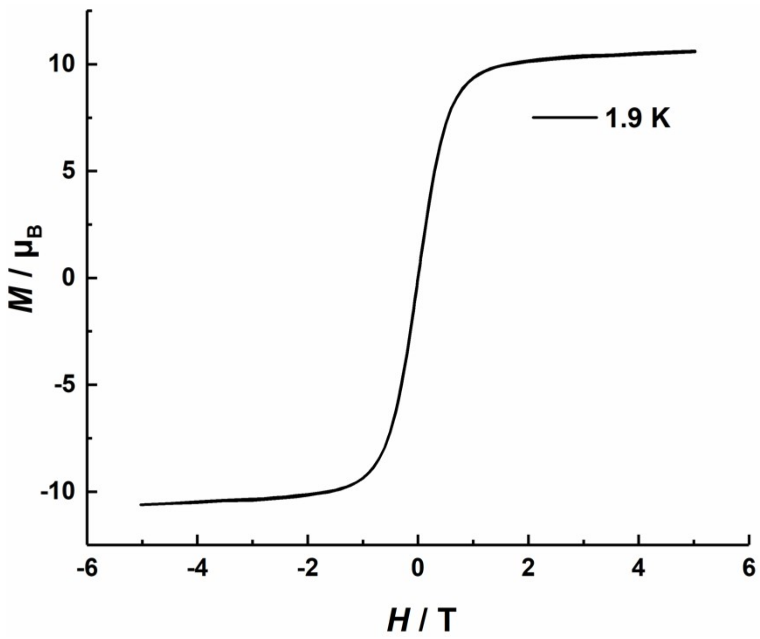

Figure S7. Variable magnetic field magnetization measurement for **2** at 1.9 K.

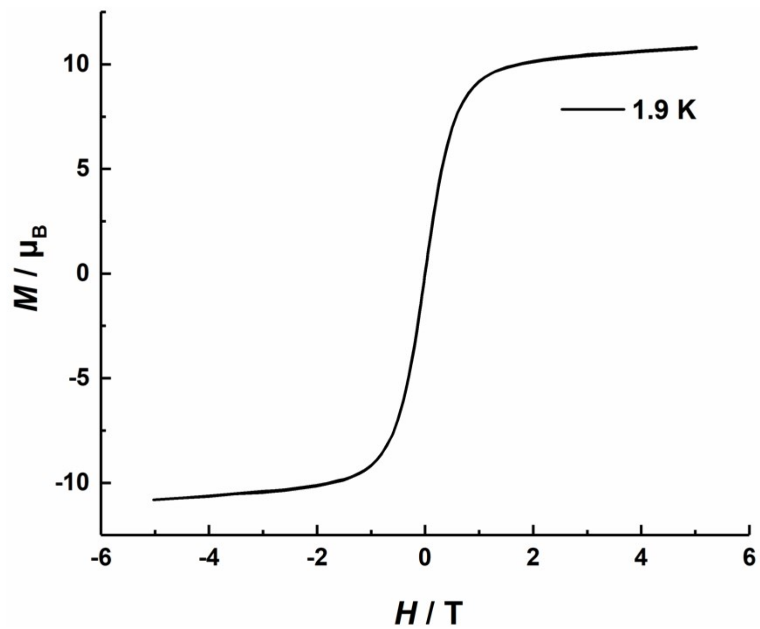

Figure S8. Variable magnetic field magnetization measurement for **3** at 1.9 K.

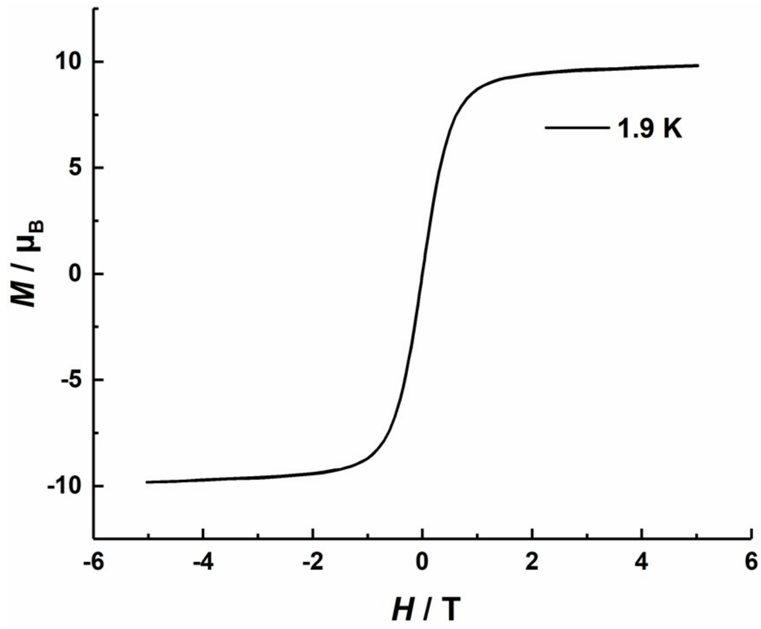

Figure S9. Variable magnetic field magnetization measurement for **4** at 1.9 K.

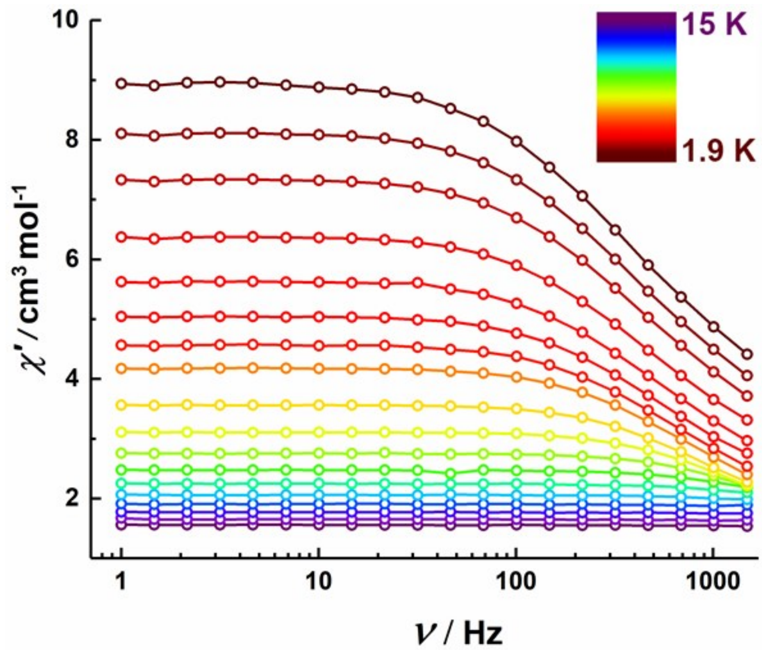

Figure S10. Frequency dependence under zero dc field of the in-phase ac susceptibility component at indicated temperature for **1**.

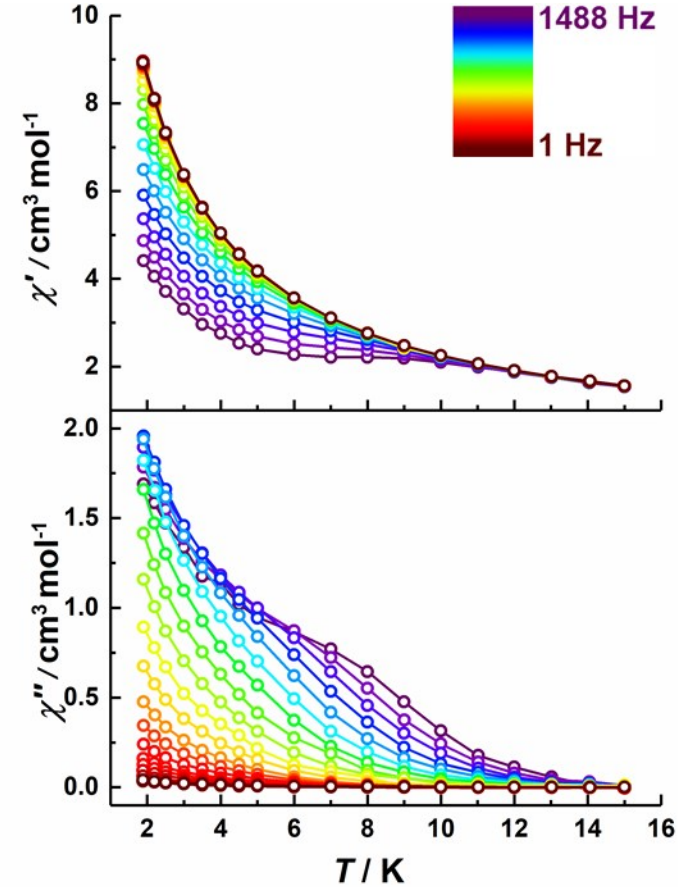

Figure S11. Temperature dependence under zero dc field of the in-phase (top) and the out-of-phase (bottom) ac susceptibility component at indicated ac frequency for **1**.

Table S3. Parameters Gained From the Fitting of Relaxation Time (τ) Versus Temperature (T^{-1}) Plots for **1**, **2** and **4**. For **3**, Parameters Gained From the e.q. (3).

compound	U_{eff} / K	τ_0 / s	τ_{QTM} / s	A / s^{-1} K^{-1}	C / s^{-1} K^{-n}	n
1	45.1	4.97×10^{-7}	6.1×10^{-4}	/	7.8×10^{-6}	9.0
2	44.2	4.14×10^{-6}	1.4×10^{-3}	258	0.34	5.4
3	1.3	2.79×10^{-5}	/	/	/	/
4	56.2	6.15×10^{-6}	2.0×10^{-3}	49	0.3	4.8

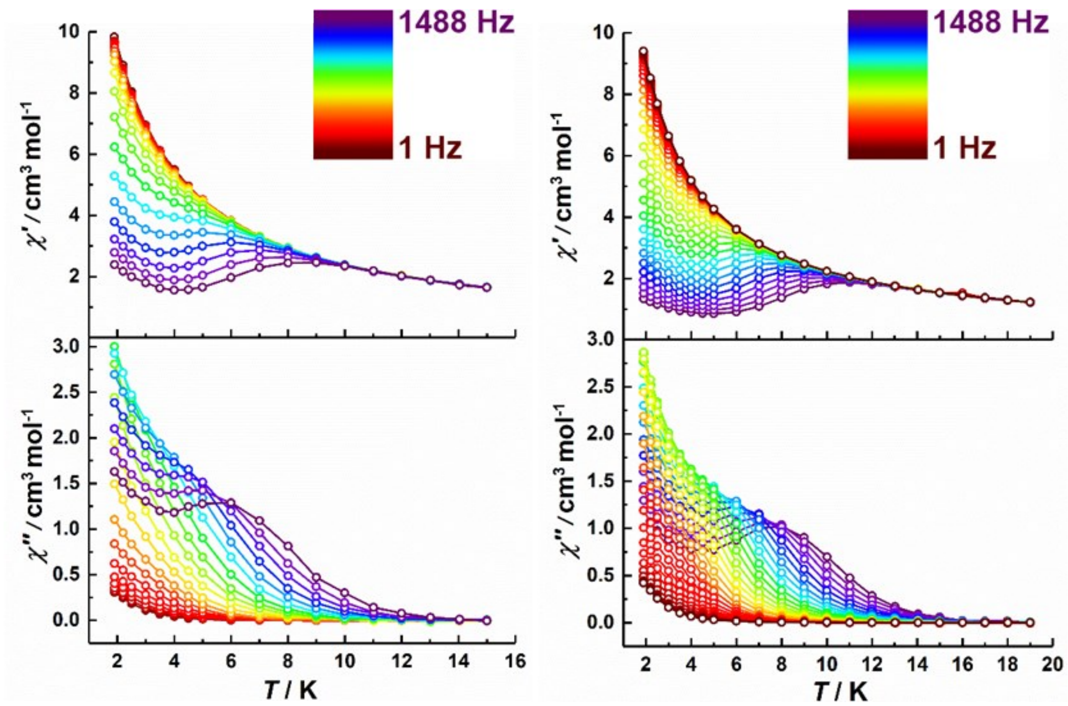

Figure S12. Temperature dependence under 500 (left) and 600 (right) Oe dc field of the in-phase (top) and the out-of-phase (bottom) ac susceptibility component at indicated ac frequency for **2** (left) and **4** (right).

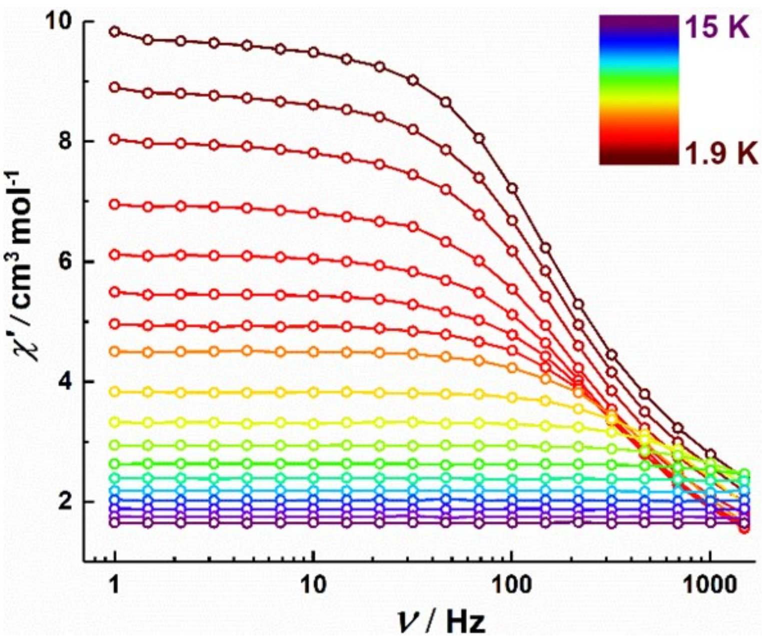

Figure S13. Frequency dependence under 600 Oe dc field of the in-phase ac susceptibility component at indicated temperature for **2**.

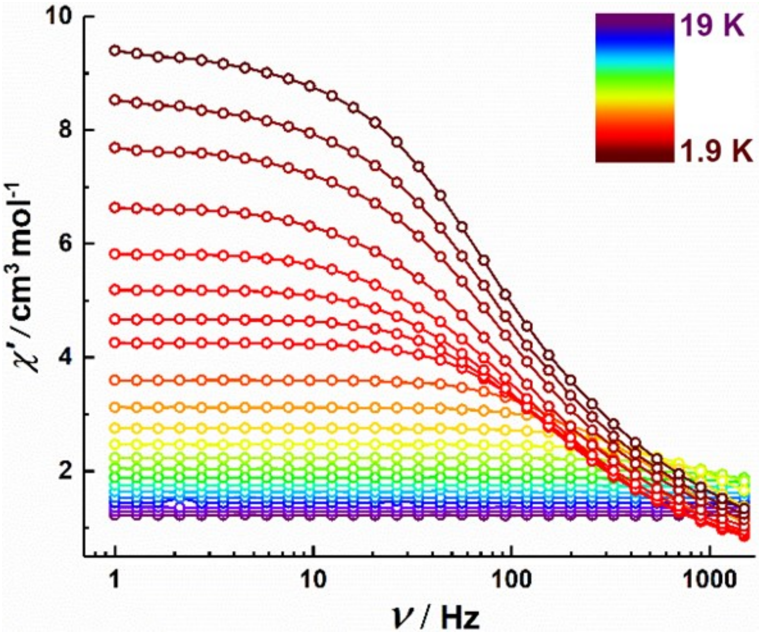

Figure S14. Frequency dependence under 500 Oe dc field of the in-phase ac susceptibility component at indicated temperature for **4**.

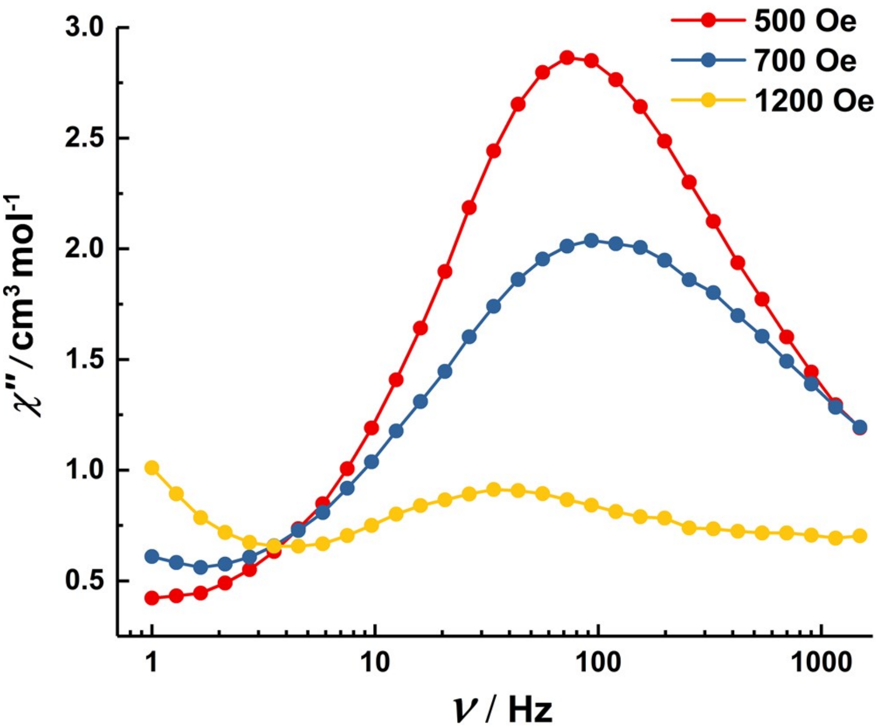

Figure S15. χ'' versus ν plot at 1.9 K under various applied dc field for **4**.

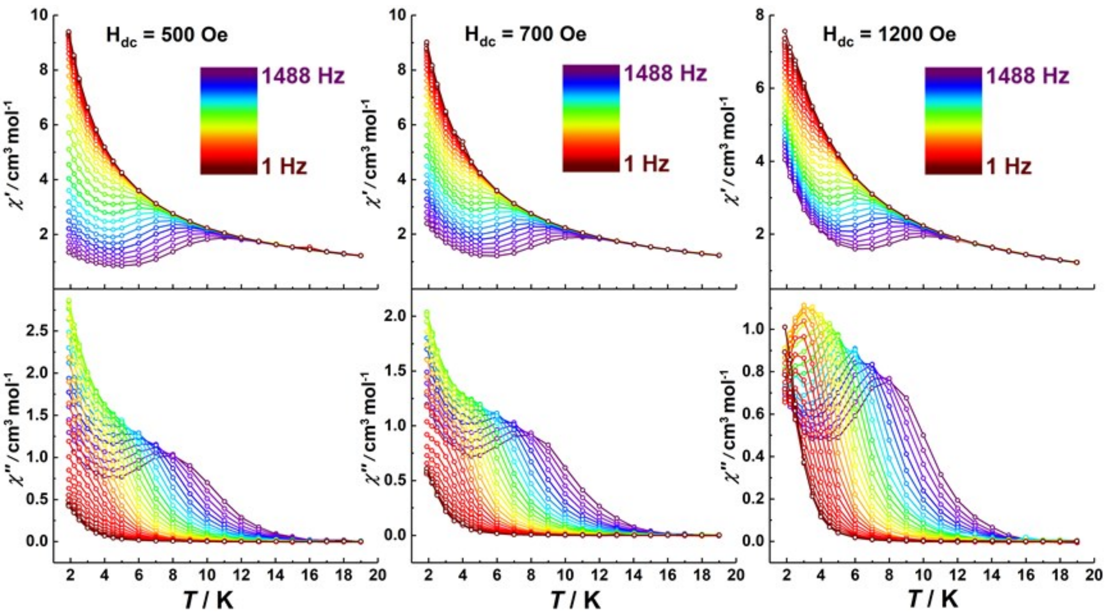

Figure S16. Temperature dependence under 500 (left), 700 (middle) and 1200 (right) Oe dc field of the in-phase (top) and the out-of-phase (bottom) ac susceptibility component at indicated ac frequency for **4**.

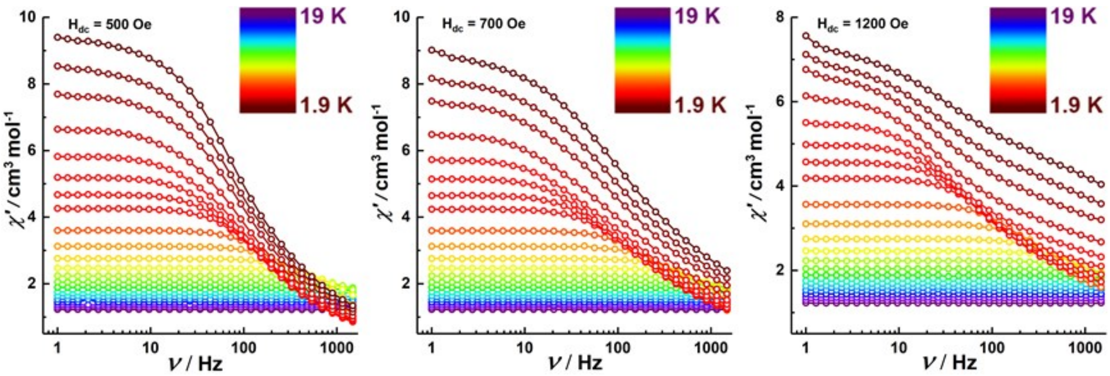

Figure S17. Frequency dependence under 500 (left), 700 (middle) and 1200 (right) Oe dc field of the in-phase ac susceptibility component at indicated temperature for **4**.

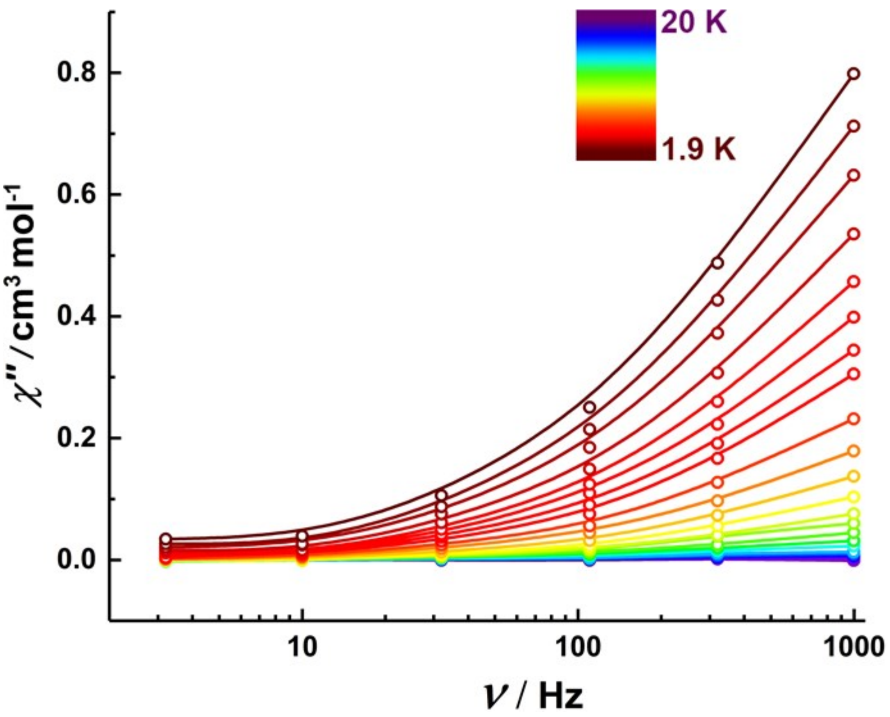

Figure S18. Frequency dependence under zero dc field of the out-of-phase ac susceptibility component at indicated temperature for **3**.

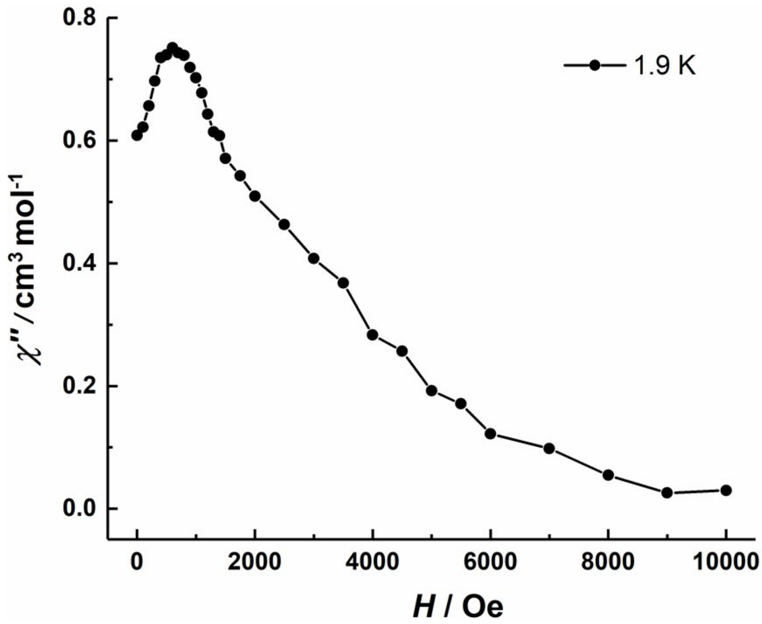

Figure S19. Field dependence of out-of-phase ac susceptibilities for **3** at 1.9 K, 997 Hz.

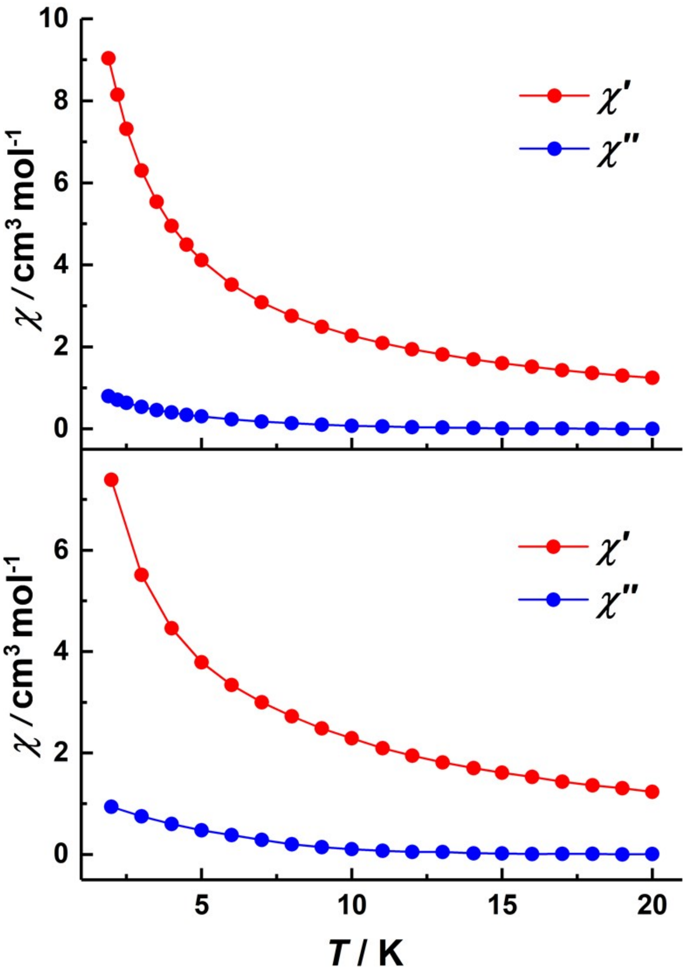

Figure S20. Temperature dependence under 0 (top) and 600 (bottom) Oe dc field of the in-phase (red) and the out-of-phase (blue) ac susceptibility component at 997 Hz for **3**.

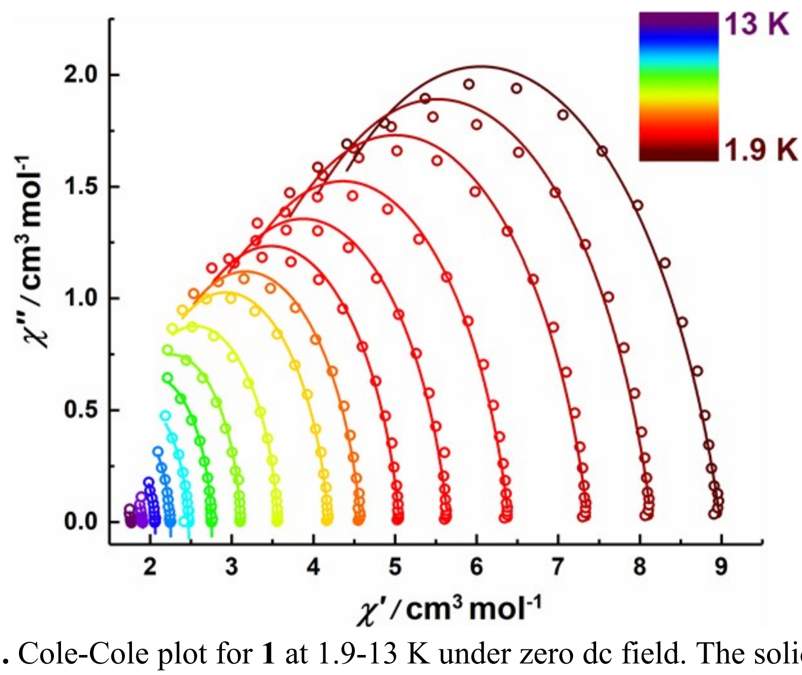

Figure S21. Cole-Cole plot for **1** at 1.9-13 K under zero dc field. The solid lines stand for the best fit using a generalized Debye model.

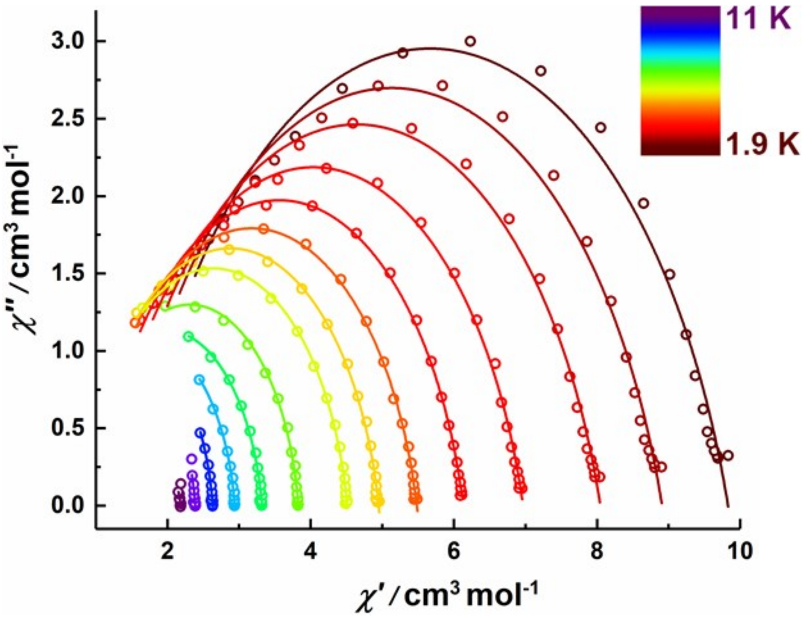

Figure S22. Cole-Cole plot for **2** at 1.9-11 K under 600 Oe applied dc field. The solid lines stand for the best fit using a generalized Debye model.

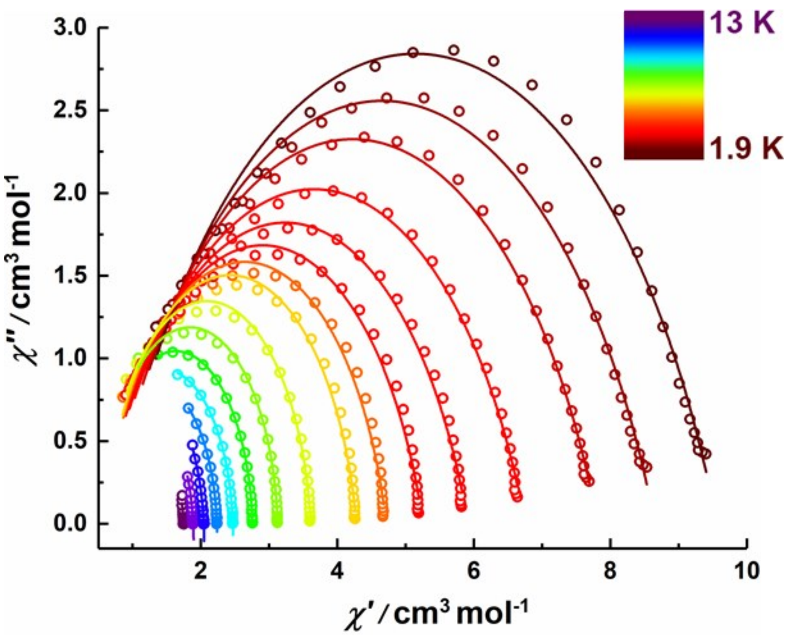

Figure S23. Cole-Cole plot for **4** at 1.9-13 K under 500 Oe applied dc field. The solid lines stand for the best fit using a generalized Debye model.